Proceedings of the 33rd European Safety and Reliability Conference (ESREL 2023)
Edited by Mário P. Brito, Terje Aven, Piero Baraldi, Marko Čepin and Enrico Zio
 Published by Research Publishing, Singapore.
doi: 10.3850/978-981-18-8071-1_P355-cd

Experimental Analysis of a Lithium-Ion Battery Pack after Long Service Life in a Conventional Electric Vehicle Considering Second-Life Applications

Tobias Scholz, Friedbert Pautzke

Electric Vehicle Institute, Bochum University of Applied Science, Germany.
E-mail: tobias.scholz@hs-bochum.de, friedbert.pautzke@hs-bochum.de

Benedikt Schmuelling

Chair of Electric Mobility and Energy Storage Systems, University of Wuppertal, Germany.
E-mail: schmuelling@uni-wuppertal.de

The mobility transformation from the classic combustion engine to the electric vehicle (EV) is the current focus of research and development. The increasing market penetration of EVs and the need for a sustainable and resource-saving energy transition make the development of second-use concepts necessary. Since the condition of the batteries after first life in an EV is mostly unknown, the batteries must be tested in or outside the vehicle before a decision can be made about re-use or recycling. For decision making, the remaining capacity and the internal resistance must be determined. Due to the unknown state of the system, the methods normally used for this must be reconsidered, as aged traction batteries behave different in comparison to new ones. Accordingly, this paper discusses the process of testing for second life (SL) applications using a conventional EV after 11 years of usage as an example. For this purpose, the classic capacitance test at various temperatures and current levels, and a modified high-pulse power characterization test (HPPC) were applied at module level. Further, conclusions on the cell behavior and reconfiguration are drawn by approximation of the characteristic voltage curve to calculate cell-to-cell capacitance differences.

Keywords: reliability, sustainability, safety, second life, traction batteries, condition assessment, battery testing.

1. Introduction

The global ramp-up of electromobility can only be sustainable if the efficient use of energy and materials is ensured. Despite steadily decreasing costs in the process chain to produce lithium-ion traction batteries since 2010, they can still account for up to 40 % of the total costs of an EV. (Shahjalal et al., 2022; Wietschel et al., 2022) After initial use in the EV, it may make sense to use the battery pack for another application, for example as stationary storage. Which can be the case if battery capacity and/or power capability are no longer suitable for the user's mobility requirements, or the traction battery has been removed due to other damage to the EV. (Börner et al., 2022; Montes et al., 2022)

Current ageing studies typically consider the percentage of remaining capacity compared to nominal capacity C_N at the Begin of life (BoL) or the percentual increase of internal resistance. The so-called State of Health (SOH_C or SOH_R), where the index describes if it is capacitance or resistance related. A remaining SOH_C of 80-70 % is in general considered End-of-Life (EoL) in the EV application (first life) , which can also be considered as a theoretical threshold for SL applications. (Kotak et al., 2021; Kremzow-Tennie et al., 2022; Podias et al., 2018). The threshold value of the resistance increase is typically assumed at 200 % of the initial resistance, The SOH_R is generally more likely used for hybrid vehicles with high-power cells. (Ecker et al., 2012; Grandjean et al., 2018) Due to the general usage of high-energy cells in conventional EVs. Original equipment manufacturer (OEM) typically define a SOH_C of 70 % as a guarantee until a defined mileage is reached or period of time has passed. (Petersen 2021; Autorevue Online Redaktion 2021) For traction batteries of electric vehicles, extensive standardized measurement methods are used to

determine the capacity and internal resistance at BoL using power electronics. The ISO 12405-4 (ISO 12405-4, 2018), which included measurement methods for high-energy and high-power traction battery systems does not include a percentage EoL characteristic value. The EoL is reached when a condition specified by the manufacturer is reached or the battery pack can no longer pass the specified test methods. The SAE J2280:2020 (SAE International, 2020) which describes the life cycle testing of electric vehicle battery modules consider a threshold of 80 % SOH_C as EoL criteria. To take all regulations into account 70 % SOH_C is assumed as the threshold value in this study.

Due to the long use in EVs, the geographical location, environment temperature as well as the specific usage profile in terms of driving and charging/fast charging, all vehicles age individually. (Guenther et al., 2021; Guo et al., 2021; Kremzow-Tennie et al., 2021) The construction and cooling of the battery in the EV, as well as production tolerances, can lead to initial but also accumulating inhomogeneous ageing within the battery pack. (Scholz et al., 2021; Schuster et al., 2016)

Therefore characterization of SL batteries tends to be a more technical and safety-critical endeavor compared to BoL batteries. (Hossain et al., 2019) This results from the different history and the unknown condition at the time of the characterization. (Börner et al., 2022) Whereby SL concepts are generally assumed to be in a SOH_C range of 80-30%. Due to this wide range, the application of standardized investigations is correspondingly complex. (Illa Font et al., 2023) Capacitance and internal resistance may have changed significantly compared to the BoL. The data sheet of the battery should serve as a basis for the design of test. However, it can be assumed that the standardized tests from the BoL characterization at the start of the SL can only be carried out with significantly reduced load scenarios. Initial tests should always be performed in the lower load segment.

Within this paper, the characterization process of the traction battery of a Peugeot iOn is presented considering SL applications and pointing out any technical and safety challenges. In addition to the pure investigation on module level, an estimation of the cell state is performed based on the results, which in this respect represents a time-efficient option for module and pack reconfiguration.

2. Data Acquisition

2.1. *Vehicle under test*

In this study a Peugeot iOn manufactured in 2011 was tested. At the time of disassembly, the vehicle had 41.200 km of mileage. The structural design of the battery is shown in Fig. 1. The traction battery consists of 88 cells connected in series (Millikin, 2008). The prismatic cells used are LEV-50 by GS Yasua. C_N is rated with 50 Ah. The nominal Voltage U_N of the battery pack is 330 V. The cell characteristics can be found in Table 1. The battery cells are divided into twelve modules. Ten modules with eight cells in series each and two modules with four cells each.

Fig. 1. Top view of the removed battery module before disassembly down to module level.

Table 1. Cell characteristics of given LEV-50 (Shinya et al., 2008)

Cell Characteristics	
Nominal voltage U_N	3.75 V
Operating voltage range	2.75 V to 4.1 V
Nominal Capacity C_N	50 Ah
Continuous current	300 A
Mass	1.7 Kg
Specific energy	109 Wh/Kg
Energy density	300 Wh/L

2.1. *Testbench setup and used hardware*

For every conducted laboratory measurement, a Keysight SL1001A battery module test system was used. Each channel provides 5 to 90 V and ± 300 A. In addition to the module voltage, the cell voltages were measured.

Fig. 3. Contacted battery modules in the climate chamber

To provide a homogenous temperature environment a Binder KB 400 climate chamber was used. For the measurements RS PRO Thermocouples Type K were applied to the cell surface. Each module and every cell temperature were measured with eight thermocouples, where four were applied on the left and four on the right site, which can be seen in Fig. 3.

2.2. *Applied measurement methods*

For the determination of the remaining capacitance and the internal resistance, ISO-12405 was used as the basis for the test procedures. The boundary conditions, such as thermal equilibrium and requirements for the measurement technology, were adopted. The process and modifications are explained below.

2.2.1. *Capacity measurement*

The program flow and the applied boundary conditions for the capacity measurement can be found in Fig. 4. In the test sequence, thermal equilibrium is awaited after every temperature change and a top-off charge is performed. Thermal equilibrium describes the state in which no temperature change of ±ΔT (0.1 °C) has occurred in the last hour. The initial charging process is always carried out at 25 °C and then the temperature is adjusted to T_{Set}. The top-off charge describes a charging process with C/3, which is carried out after a temperature change to compensate any loss of charge. A discharge with 1.0 C corresponds to a complete discharge within one hour, which in this application refers to C_N and corresponds accordingly to a current flow of 50 A.

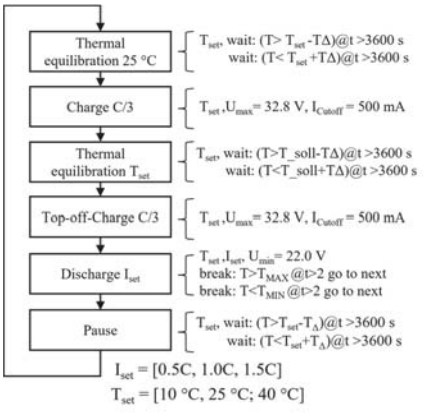

Fig. 4. Test procedure of the capacity measurement

The termination conditions correspond to the regular charging process. The measurement curve and the corresponding temperature control can be found in Fig. 5.

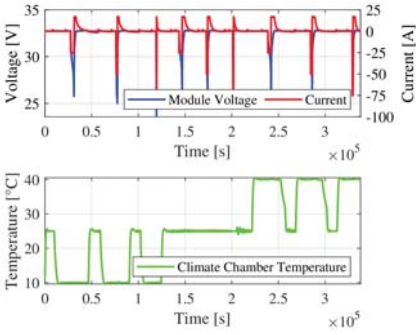

Fig. 5. Test procedure of the capacity measurement

Each module was tested in advance at 25 °C and a discharge rate of C/3, followed by a series of tests at 10 °C, 25 °C and 40 °C at 0.5 C, 1.0 C and 1.5 C, respectively. Unlike ISO 12405, in which a capacitance measurement is first performed to determine the rated capacitance, all measured quantities here are related to C_N, which allows better comparability with other studies.

2.1.3. *Measurement of the internal resistance*

Unlike the application of the ISO 12405 approach, some adjustments had to be made to the test sequence when applied to the aged traction batteries. The first step was to increase the number of SOC values approached. The program flow and the applied boundary

conditions for the capacity measurement can be found in Fig. 6.

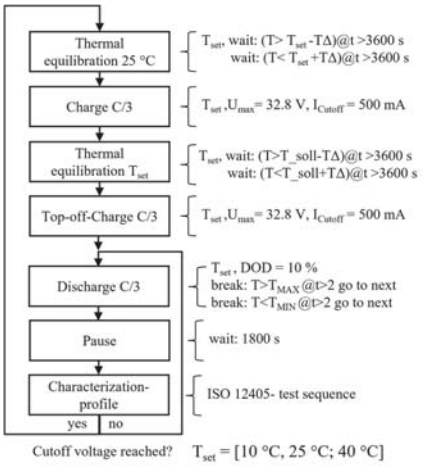

Fig. 6. Test procedure of the resistance measurement

Due to the unknown initial condition, a resistance test was performed every 10 % until 60 % and then every 5 % in relation to C_N. The SOC is calculated, using coulomb counting according to Eq. (1).

$$SOC(t) = SOC(t_0) + \frac{\int_{t_0}^{t_0+\tau} I\, d\tau}{C_N} * 100\% \qquad (1)$$

The measurement curve and the corresponding temperature control can be found in Fig. 7.

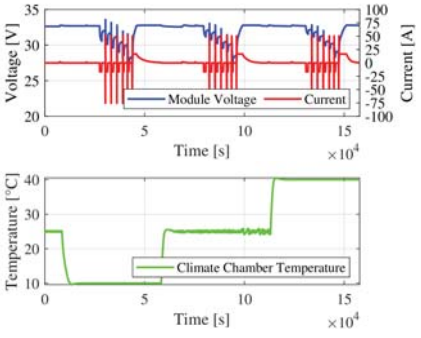

Fig. 7. Test procedure of the capacity measurement

Due to reaching the end-of-charge and end-of-discharge (EOD) voltage when using the currents specified in ISO 12405, these had to be adjusted in the test sequence, otherwise no complete measurement could be performed. In the process, the maximum discharge pulse current was reduced from 300 A to 125 A and the maximum charge current from 125 A (for 10-40 °C) to 50 A.

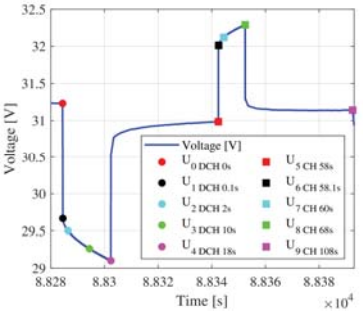

Fig. 8. Test procedure of the resistance measurement

The measurement times and general procedure for determining the internal resistance were taken from ISO12405. Fig. 8 and Table 2 contain the time points and the corresponding calculations used.

Table 2. Resistance calculations based on adapted ISO12405 specifications with lowered currents.

t	V		I	Equation
0s	U_0	I_0	0	
0.1s	U_1	I_1	-125 A	$R_{i0.1s,dch} = (U_0-U_1)/ I_1$
2s	U_2	I_2	-125 A	$R_{i2s,dch} = (U_0-U_2)/ I_2$
10s	U_3	I_3	-125 A	$R_{i10s,dch} = (U_0-U_3)/ I_3$
18s	U_4	I_4	-125 A	$R_{i18s,dch} = (U_0-U_4)/ I_4$
58s	U_5	I_5	0	$R_{idch} = (U_5-U_4)/ I_4$
58.1s	U_6	I_6	75 A	$R_{i0.1s,cha} = (U_5-U_6)/ I_6$
60s	U_7	I_7	75 A	$R_{i2s,cha} = (U_5-U_7)/ I_8$
68s	U_8	I_8	75 A	$R_{i10s,cha} = (U_5-U_8)/ I_8$
108s	U_9	I_9	0	$R_{i,cha} = (U_9-U_8)/ I_8$

3. Calculation of Cell-to-Cell Variation

Measurements at module level save time and measurement capacities compared to cell level measurements. The results offer a more accurate result than at pack level, however, just as at pack level, the worst cell limits the module capacity. Another advantage to battery pack analysis is the voltage level lower than 60 V, which reduces the qualification requirements for the personal. (Popp et al., 2021) This makes further differentiation of the individual cells for

potential reconfiguration difficult. Therefore, it makes sense to further investigate the cell capacity differences based on a UI characteristic curve. Since the C/3 voltage curve is classically used as a reference for determining the SOH_C, a polynomial function was used to approximate the cell voltage behavior to determine any differences in capacitance. The approximation of the voltage by means of an n-th order polynomial is a common method, although other functions are also suitable, depending on the data basis. (Chen et al., 2013; Scholz et al., 2018; Zhang et al., 2018)

$$U(x) = a_1x^7 + a_2x^6 + a_3x^5 + a_4x^4 + a_5x^3 + a_6x^2 + a_7x + a_8 \quad (2)$$

In this work, the best results were obtained with a 7th order polynomial according to Eq. (2). A voltage function over the discharged capacitance x was chosen to calculate the cell-to-cell capacitance differences based on this. The coefficients are $a_1 = -0.03484$, $a_2 = -0.05795$, $a_3 = 0.8822$, $a_4 = 0.1589$, $a_5 = -0.04845$, $a_6 = -0.133$, $a_7 = -0.1179$ and , $a_8 = 3.934$, which were estimated with the least square method. The RMSE is 0.0078 and the R-Square value is 0.9988. The approximation results can be found in Fig. 9.

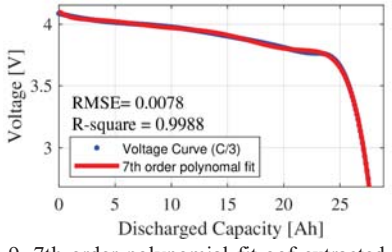

Fig. 9. 7th order polynomial fit oof extracted voltage values.

To calculate the capacity differences, the usable capacity of the cells remaining in the module, which have not reached EOD voltage, was then determined using the voltage curve as a function-table.

4. Results

4.1. Results of the capacitance measurement

Fig. 10 shows the results of the capacitance measurement and the associated relative capacitance at different discharge rates and temperatures. The strong influence of the discharge current on the usable capacity can be attributed to the strong increased internal resistance, which leads to a fast reaching of the EOD voltage due to an increased voltage drop. A summary of the averaged results can be found in Table 3. Where σ describes the standard deviation.

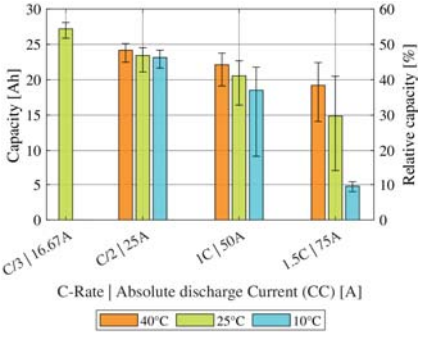

Fig. 10. Determined capacity at different temperatures and current levels.

Table 3. Results of the capacitance Measurement

	C-Rate	Mean [Ah]	Min. [Ah]	Max. [Ah]	σ [Ah]
25°C	C/3	27.18	25.87	28.08	0.66
	C/2	23.42	21.09	24.53	1.23
	1.0C	20.55	16.42	22.68	2.27
	1.5C	14.87	6.98	20.49	5.23
10°C	C/2	23.14	21.65	24.17	1.22
	1.0C	18.51	9.19	21.78	4.19
	1.5C	4.78	4.00	5.40	0.47
40°C	C/2	24.16	22.48	25.11	0.97
	1.0C	22.11	19.12	23.76	1.70
	1.5C	19.21	14.11	22.43	2.91

The calculation of the SOH_C is carried out with the results of the C/3 capacitance measurement at 25 °C. The SOH_C is determined using Eq. (3).

$$SOH_C = \frac{C_{C/3}}{C_N} * 100\% \quad (3)$$

This corresponds to an averaged SOH_C of all tested modules of 54.36 %.

4.1. Results of the resistance measurement

Fig. 11 shows the determined 10-second internal resistances plotted against the SOC at different temperatures. Averaged a resistance increase of

41.9 % takes place between 40 °C and 25 °C. Between 25 °C and 10 °C, the resistance increases by 52.9 %. This illustrates the strong influence of the ambient temperature on the performance of the battery in the vehicle and potential future applications. To achieve a higher comparability of the results, the SOC here refers to the nominal capacity, thus a SOC of 50 % corresponds to a discharged capacity of 25 Ah. The lower the state of charge, the higher the determined resistance, but also the deviation between the results, which can be explained by the inhomogeneity of the modules.

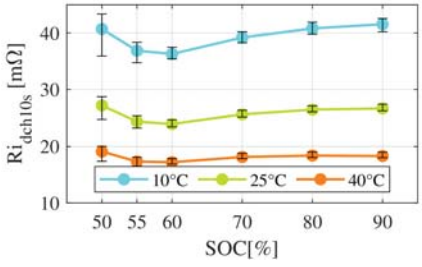

Fig. 11. Determined 10 second discharge resistance at different temperatures and current levels.

A summary of the averaged results for the 10-second discharge and charge resistance can be found in Table 4. It can be seen that the aging processes not only have a negative effect on the performance in driving operation, but also on the efficiency in the charging process.

Table 4. Results of the resistance Measurement averaged over all SOC-Values

		Mean [mΩ]	Min. [mΩ]	Max. [mΩ]	⌀σ [mΩ]
$R_{i10s,dch}$	25°C	25.66	23.15	28.72	0.73
	10°C	39.24	34.75	43.37	1.29
	40°C	18.08	16.51	20.03	0.55
$R_{i10s,cha}$	25°C	28.69	23.10	36.91	0.80
	10°C	46.17	33.65	58.94	1.46
	40°C	19.30	16.70	25.05	0.56

There is no information on the DC resistance in the manufacturer's data sheet, which makes a direct comparison to determine the SOH_R impossible. According to the literature, however, an internal resistance of 11.1-13.6 mΩ on average can be assumed. (De Vroey et al., 2013; Idaho National Laboratory, 2014; Nguyen et al., 2021) This leads to a corresponding SOH_R of 188.7-231.2 % with Eq. (4) considering the averaged resistance at 25°C of 25.66 mΩ.

$$SOH_R = \frac{R_{mean}}{R_{BoL}} * 100\% \quad (4)$$

4.3 Results of the cell-to-cell variation analysis

To make a statement about capacity differences between the individual cells within a module. Based on the characteristic voltage curve, the remaining capacity of the individual cells that have not yet reached the EOD voltage in the module test was determined. Fig. 12 shows the results of the analysis based on the C/3 capacity measurement. The black line describes the SOH_C corresponding to the measured capacitance, which is defined by the weakest cell in the module. The individual bars describe the capacity of the individual cells.

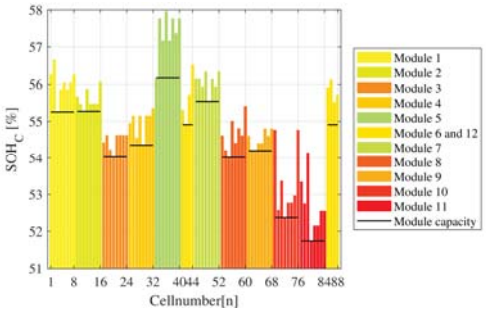

Fig. 12. Cell Ranking based on curve fitting results.

Table 5 compares the results from Fig.12 at pack, module, and cell level. The worst cell significantly limits the capacity of the respective module and therefore the entire pack. The maximum SOH_C difference between the best and worst cell is 6.21 %. The worst cell is 3.28 % below the average.

Table 5. Comparison of the results on Pack, Module and Cell level

	Mean [%/Ah]	Min. [%/Ah]	Max. [%/Ah]	σ [%/Ah]
Pack	-	-	51.75 25.87	-
Module	54.35 27.18	51.75 25.87	56.16 28.08	1.32 0.66
Cell	55.03 27.52	51.75 25.87	57.96 28.98	1.36 0.68

5. Summary and outlook

In summary, this paper demonstrated the approach of testing for SL applications using a conventional EV as an example and presented the results. The SOH, which is not known in advance, has a major influence in terms of resistance and capacitance testing. There is a great uncertainty at which SOH level the batteries can be used for SL applications because the mobility requirements of the users are different. However, it can be assumed that the smaller the battery, the faster the range restrictions are felt, which possibly leads to faster transfer into SL applications. It has been shown that module level testing allows meaningful results without initial further disassembly. It was also shown that the approximation of the voltage behavior and estimation of the cell capacity is useful, especially regarding welded modules, which are more complex to disassemble. Regarding the reconfiguration of the modules or the pack, since the weakest cell at all levels determines the capacity, it appeared that it can be useful to swap the cells among themselves in the modules. Goal of future work will be the economic and technical scalability of such methods to larger vehicle fleets.

Acknowledgement

The authors would like to thank Voltavision GmbH for providing the measurement equipment and assistance in carrying out the measurements in the laboratory. Furthermore, the authors would like to thank the German Federal Ministry of Education and Research (project UniZub, 03XP0500D), and Bochum University of Applied Science for financially supporting parts of this work.

References

Autorevue Online Redaktion, 2021. Elektroautos Marktübersicht: Alle E-Modelle, Daten und Tests [Reichweiten + Preise] [WWW Document]. autorevue.at. URL https://autorevue.at/autowelt/alle-elektroautos-preise-testberichte-daten (accessed 2.17.22).

Börner, M.F., Frieges, M.H., Späth, B., Spütz, K., Heimes, H.H., Sauer, D.U., Li, W., 2022. Challenges of second-life concepts for retired electric vehicle batteries. Cell Reports Physical Science 3, 101095. https://doi.org/10.1016/j.xcrp.2022.101095

Chen, Z., Fu, Y., Mi, C.C., 2013. State of Charge Estimation of Lithium-Ion Batteries in Electric Drive Vehicles Using Extended Kalman Filtering. IEEE Trans. Veh. Technol. 62, 1020–1030. https://doi.org/10.1109/TVT.2012.2235474

De Vroey, L., Jahn, R., El Baghdadi, M., Van Mierlo, J., 2013. Plug-to-wheel energy balance-results of a two years experience behind the wheel of electric vehicles, in: 2013 World Electric Vehicle Symposium and Exhibition (EVS27). Presented at the 2013 27th International World Electric Vehicle Symposium and Exhibition (EVS27), IEEE, Barcelona, Spain, pp. 1–5. https://doi.org/10.1109/EVS.2013.6914803

Ecker, M., Gerschler, J.B., Vogel, J., Käbitz, S., Hust, F., Dechent, P., Sauer, D.U., 2012. Development of a lifetime prediction model for lithium-ion batteries based on extended accelerated aging test data. Journal of Power Sources 215, 248–257. https://doi.org/10.1016/j.jpowsour.2012.05.012

Grandjean, T., Groenewald, J., McGordon, A., Widanage, W., Marco, J., 2018. Accelerated Internal Resistance Measurements of Lithium-Ion Cells to Support Future End-of-Life Strategies for Electric Vehicles. Batteries 4, 49. https://doi.org/10.3390/batteries4040049

Guenther, L.H., Scholz, T., Pautzke, F., Fechtner, H., Schmuelling, B., Schelte, N., Severengiz, S., Hinz, M., Bracke, S., 2021. Reliability Engineering of Electric Vehicle Powertrains: Data Collection and Analysis Based on Products in the Usage Phase, in: Proceedings of the 31st European Safety and Reliability Conference (ESREL 2021). Presented at the Proceedings of the 31st European Safety and Reliability Conference, Research Publishing Services, pp. 2573–2580. https://doi.org/10.3850/978-981-18-2016-8_183-cd

Guo, J., Li, Y., Pedersen, K., Stroe, D.-I., 2021. Lithium-Ion Battery Operation, Degradation, and Aging Mechanism in Electric Vehicles: An Overview. Energies 14, 5220. https://doi.org/10.3390/en14175220

Hossain, E., Murtaugh, D., Mody, J., Faruque, H.M.R., Haque Sunny, Md.S., Mohammad, N., 2019. A Comprehensive Review on Second-Life Batteries: Current State, Manufacturing Considerations, Applications, Impacts, Barriers & Potential Solutions, Business Strategies, and Policies. IEEE Access 7, 73215–73252. https://doi.org/10.1109/ACCESS.2019.2917859

Idaho National Laboratory, 2014. BEV Battery Testing Results - 2012 Mitsubishi i-Miev - VIN 4550.

Illa Font, C.H., Siqueira, H.V., Machado Neto, J.E., Santos, J.L.F. dos, Stevan, S.L., Converti, A., Corrêa, F.C., 2023. Second Life of Lithium-Ion Batteries of Electric Vehicles: A Short Review

and Perspectives. Energies 16, 953. https://doi.org/10.3390/en16020953

ISO 12405-4, 2018. ISO 12405-4 Electrically propelled road vehicles - Test specification for lithium-ion traction battery packs and systems - Part 4: Performance testing. Geneva, Switzerland.

Kotak, Y., Marchante Fernández, C., Canals Casals, L., Kotak, B.S., Koch, D., Geisbauer, C., Trilla, L., Gómez-Núñez, A., Schweiger, H.-G., 2021. End of Electric Vehicle Batteries: Reuse vs. Recycle. Energies 14, 2217. https://doi.org/10.3390/en14082217

Kremzow-Tennie, S., Pautzke, F., Mecit, H., Scholz, T., Schmuelling, B., 2021. A Suggestion Towards Improving Electric Vehicle Fast Charging, in: Proff, H. (Ed.), Making Connected Mobility Work. Springer Fachmedien Wiesbaden, Wiesbaden, pp. 251–261. https://doi.org/10.1007/978-3-658-32266-3_14

Kremzow-Tennie, S., Scholz, T., Pautzke, F., Popp, A., Fechtner, H., Schmuelling, B., 2022. A Comprehensive Overview of the Impacting Factors on a Lithium-Ion-Battery's Overall Efficiency. Power Electronics and Drives 7, 9–28. https://doi.org/10.2478/pead-2022-0002

Millikin, M., 2008. The Battery Pack for Mitsubishi's i MiEV [WWW Document]. Greencarcongress.com. URL https://www.greencarcongress.com/2008/05/the-battery-pac.html

Montes, T., Etxandi-Santolaya, M., Eichman, J., Ferreira, V.J., Trilla, L., Corchero, C., 2022. Procedure for Assessing the Suitability of Battery Second Life Applications after EV First Life. Batteries 8, 122. https://doi.org/10.3390/batteries8090122

Nguyen, H.-L.T., Nguyễn, B.-H., Vo-Duy, T., Trovão, J.P.F., 2021. A Comparative Study of Adaptive Filtering Strategies for Hybrid Energy Storage Systems in Electric Vehicles. Energies 14, 3373. https://doi.org/10.3390/en14123373

Petersen, L.H., 2021. Elektroauto: Diese Akku-Garantien geben die Hersteller [WWW Document]. autobild.de. URL https://www.autobild.de/artikel/elektroauto-akku-hersteller-garantie-lebensdauer-porsche-tesla-vw-20343233.html (accessed 2.17.22).

Podias, A., Pfrang, A., Di Persio, F., Kriston, A., Bobba, S., Mathieux, F., Messagie, M., Boon-Brett, L., 2018. Sustainability Assessment of Second Use Applications of Automotive Batteries: Ageing of Li-Ion Battery Cells in Automotive and Grid-Scale Applications. WEVJ 9, 24. https://doi.org/10.3390/wevj9020024

Popp, A., Fechtner, H., Schmuelling, B., Kremzow-Tennie, S., Scholz, T., Pautzke, F., 2021. Battery Management Systems Topologies: Applications : Implications of different voltage levels, in: 2021 IEEE 4th International Conference on Power and Energy Applications (ICPEA). Presented at the 2021 IEEE 4th International Conference on Power and Energy Applications (ICPEA), IEEE, Busan, Korea, Republic of, pp. 43–50. https://doi.org/10.1109/ICPEA52760.2021.9639285

SAE International, 2020. Life Cycle Testing of Electric Vehicle Battery Modules.

Scholz, T., Hellwig, M., Pautzke, F., 2018. Algorithm for Parameter Identification of Lithium-Ion Batteries, in: VDI Wissensforum GmbH (Ed.), SIMVEC – Simulation Und Erprobung in Der Fahrzeugentwicklung. VDI Verlag, pp. 389–398. https://doi.org/10.51202/9783181023334-389

Scholz, T., Kremzow-Tennie, S., Pautzke, F., Fechtner, H., Popp, A., Schmuelling, B., 2021. Analysis of Cell-to-Cell Variation in a Battery Pack after Long Service Life Using Parameter Identification, in: 2021 IEEE 4th International Conference on Power and Energy Applications (ICPEA). Presented at the 2021 IEEE 4th International Conference on Power and Energy Applications (ICPEA), IEEE, Busan, Korea, Republic of, pp. 38–42. https://doi.org/10.1109/ICPEA52760.2021.9639370

Schuster, S.F., Brand, M.J., Campestrini, C., Gleissenberger, M., Jossen, A., 2016. Correlation between capacity and impedance of lithium-ion cells during calendar and cycle life. Journal of Power Sources 305, 191–199. https://doi.org/10.1016/j.jpowsour.2015.11.096

Shahjalal, M., Roy, P.K., Shams, T., Fly, A., Chowdhury, J.I., Ahmed, Md.R., Liu, K., 2022. A review on second-life of Li-ion batteries: prospects, challenges, and issues. Energy 241, 122881. https://doi.org/10.1016/j.energy.2021.122881

Shinya, K., Koichi, N., Jun-ichi, T., Teruo, S., 2008. Development of Large-sized Lithium-ion Cell "LEV40" and Its battery Module "LEV50-4" for Electric Vehicle (Technical Report).

Wietschel, M., Thielmann, A., Plötz, P., Gnann, T., Sievers, L., Breitschopf, B., Doll, C., Moll, C., 2022. Perspektiven des Wirtschaftsstandorts Deutschland in Zeiten zunehmender Elektromobilität. https://doi.org/10.24406/PUBLICA-FHG-298570

Zhang, R., Xia, B., Li, B., Cao, L., Lai, Y., Zheng, W., Wang, H., Wang, W., Wang, M., 2018. A Study on the Open Circuit Voltage and State of Charge Characterization of High Capacity Lithium-Ion Battery Under Different Temperature. Energies 11, 2408. https://doi.org/10.3390/en11092408